

Empirical Approach to Estimate Net Ecosystem Exchange Using High Frequency Mesonet Observations across Potential Switchgrass Establishment Landscapes in Oklahoma

Kundan Dhakal¹, Vijaya Gopal Kakani², Pradeep Wagle³, and Sonisa Sharma⁴

¹Oklahoma State University

²Oklahoma State University Stillwater

³USDA-ARS Grazinglands Research Laboratory

⁴Noble Research Institute

November 22, 2022

Abstract

Monitoring net ecosystem carbon dioxide (CO₂) exchange (NEE) using eddy covariance (EC) flux towers is quite common, but the measurements are valid at the scale of tower footprints. Alternative ways to quantify and extrapolate EC-measured NEE across potential production areas have not been explored in detail. To address this need, we used NEE measurements from a switchgrass (*Panicum virgatum* L.) ecosystem and detailed meteorological measurements from the Oklahoma Mesonet and developed empirical relationships for quantifying seasonal (April to October) NEE across potential switchgrass establishment landscapes in Oklahoma, USA. We identified ensemble area for potential switchgrass expansion regions and created thematic maps of switchgrass productivity using geostatistics and GIS routines. The purpose of this study was not to calibrate the model for estimating NEE in the future but to explore if model parametrizations based on high temporal frequency meteorological forcing can be used to construct reliable estimates of NEE for evaluating the source-sink status of organic carbon. Based on EC measurements, empirical models, a) rectangular hyperbolic light-response curve and b) temperature response functions, were fitted to estimate gross primary production (GPP) and ecosystem respiration (ER) on a seasonal scale. Model performance validated by comparing EC-measured seasonal NEE for three years showed good-to-strong agreement ($0.29 < R^2 < 0.91$; $p < 0.05$). Additionally, total seasonal NEE estimates were validated with measured biomass data in three additional locations. The estimated seasonal average net ecosystem production (NEP = -NEE) was 3.97 ± 1.92 (S.D.) Mg C ha⁻¹. However, results based on a simple linear model suggested significant differences in NEP between contrasting climatic years. Overall, the results from this study indicate that this new scaling-up exercise involving high temporal resolution meteorological data may be a helpful tool for assessing spatiotemporal heterogeneity of switchgrass production and the potential of switchgrass fields to sequester carbon in the Southern Great Plains of the United States.

Empirical Approach to Estimate Net Ecosystem Exchange Using High Frequency Mesonet Observations across Potential Switchgrass Establishment Landscapes in Oklahoma

1 **Kundan Dhakal^{1,2}, Vijaya Gopal Kakani^{1*}, Pradeep Wagle³, Sonisa Sharma²**

2 ¹Plant and Soil Sciences, Oklahoma State University, Stillwater, OK, USA

3 ²Noble Research Institute, LLC, Ardmore, OK, USA

4 ³USDA-ARS, El Reno, OK, USA

5 *** Correspondence:**

6 Vijaya Gopal Kakani

7 v.g.kakani@okstate.edu

8 **Keywords: net ecosystem exchange, switchgrass, eddy covariance, empirical**

9 **Abstract**

10 Monitoring net ecosystem carbon dioxide (CO₂) exchange (NEE) using eddy covariance (EC) flux
11 towers is quite common, but the measurements are valid at the scale of tower footprints. Alternative
12 ways to quantify and extrapolate EC-measured NEE across potential production areas have not been
13 explored in detail. To address this need, we used NEE measurements from a switchgrass (*Panicum*
14 *virgatum* L.) ecosystem and detailed meteorological measurements from the Oklahoma Mesonet and
15 developed empirical relationships for quantifying seasonal (April to October) NEE across potential
16 switchgrass establishment landscapes in Oklahoma, USA. We identified ensemble area for potential
17 switchgrass expansion regions and created thematic maps of switchgrass productivity using
18 geostatistics and GIS routines. The purpose of this study was not to calibrate the model for estimating
19 NEE in the future but to explore if model parametrizations based on high temporal frequency
20 meteorological forcing can be used to construct reliable estimates of NEE for evaluating the source-
21 sink status of organic carbon. Based on EC measurements, empirical models, a) rectangular
22 hyperbolic light-response curve and b) temperature response functions, were fitted to estimate gross
23 primary production (GPP) and ecosystem respiration (ER) on a seasonal scale. Model performance
24 validated by comparing EC-measured seasonal NEE for three years showed good-to-strong
25 agreement ($0.29 < R^2 < 0.91$; $p < 0.05$). Additionally, total seasonal NEE estimates were validated
26 with measured biomass data in three additional locations. The estimated seasonal average net
27 ecosystem production (NEP = -NEE) was 3.97 ± 1.92 (S.D.) Mg C ha⁻¹. However, results based on a
28 simple linear model suggested significant differences in NEP between contrasting climatic years.
29 Overall, the results from this study indicate that this new scaling-up exercise involving high temporal
30 resolution meteorological data may be a helpful tool for assessing spatiotemporal heterogeneity of
31 switchgrass production and the potential of switchgrass fields to sequester carbon in the Southern
32 Great Plains of the United States.

33

34 1 Introduction

35 Fossil fuel combustion has been identified as a primary carbon dioxide (CO₂) emission source and a
36 key factor in the mounting human-induced climate crises. The development of carbon-neutral or
37 carbon-negative alternative fuel is an urgent global priority to curtail the increasing consumption of
38 fossil fuel and mitigate the threats of the climate crisis. Various cellulosic biofuel species are
39 proposed as a cornerstone of a low-carbon economy with the potential to displace or reduce
40 petroleum consumption for transportation (Robertson *et al.*, 2017). Unfortunately, legislative
41 initiatives on biofuel production have expanded grain-based ethanol production and garnered
42 negative attention due to risks associated with nitrous oxide emissions, nitrate pollution, soil carbon
43 loss (Gelfand *et al.*, 2013), and food security (Demirer *et al.*, 2012). Instead, opting for perennial
44 exemplary biomass crops such as switchgrass (*Panicum virgatum* L.), miscanthus (*Miscanthus* ×
45 *giganteus*), and hybrid poplar trees (*Populus spp.*) would be a better choice for future energy
46 portfolios because of their substantial energy return on investment (Ohlrogge *et al.*, 2009).

47 Various policies and incentives (e.g., the European Union’s Renewable Energy Directive
48 (2018/2001) and the U.S. Energy Independence and Security Act, 2007) are in place currently to
49 encourage biofuel production and development. Relatedly, the enactment of the Biomass Crop
50 Assistance Program (BCAP) in 2008 was aimed to incentivize biomass for bioenergy production. To
51 achieve energy independence from foreign oil, the U.S. Energy Independence and Security Act,
52 2007, has mandated the production of 16 billion gallons (1 gallon = 3.785 liters) of cellulosic ethanol
53 by 2022. The most recent 2016 Billion-Ton Report from the U.S. Department of Energy has
54 identified willow (*Salix spp.*), miscanthus, and switchgrass as perennial feedstocks with the potential
55 for profitable production (Langholtz, 2016).

56 Switchgrass is a productive, perennial C₄ grass native to the tallgrass prairie regions of the U.S. and
57 one of the promising model energy crops for bioenergy feedstock (Wright, 2007). It is a dual-purpose
58 forage and biofuel feedstock, which requires minimal management. It is effective at storing soil
59 organic carbon, even below depths greater than 30 cm, due to its prolific and deeper root systems
60 (Lee *et al.*, 2007, Liebig *et al.*, 2005). Switchgrass has larger potential for greenhouse gas sinks
61 compared to cultivated croplands (Adler *et al.*, 2007). Ecologically, switchgrass is dominant in the
62 central Great Plains region and renders various ecosystem services, that include but are not limited to,
63 livestock forage, nitrate-nitrogen leaching mitigation (Brandes *et al.*, 2017, Griffiths *et al.*, 2021),
64 provision for wildlife habitat (Marshall *et al.*, 2017), phytoremediation (Guo *et al.*, 2019, Shrestha *et al.*,
65 2019), and wind and water erosion protection (Liebig *et al.*, 2005). Long-term data have
66 demonstrated the feasibility of switchgrass for liquid fuel production across a broad geographic
67 region of the U.S. (Mitchell *et al.*, 2014).

68 As the Agriculture Improvement Act of 2018 has reauthorized the extension of the Conservation
69 Reserve Program, production of switchgrass is likely to occur in the marginally productive land,
70 minimizing the competition with other field crops (Bigelow *et al.*, 2020). The Great Plains of the
71 U.S. has the potential to become a pivotal location for lignocellulosic feedstock production
72 (Martinez-Feria & Basso, 2020). Although the feasibility of switchgrass for biofuel production has
73 been demonstrated for the U.S. (Mitchell *et al.*, 2014), the existing scientific literature is not yet rich
74 enough to provide information on switchgrass productivity and its carbon sink potential across large
75 geographical and temporal scales (Behrman *et al.*, 2013). Lately, there has been a growing interest in
76 studying carbon dynamics in switchgrass to understand its potential to offset anthropogenic
77 greenhouse gases and make switchgrass a promising bioenergy crop (Eichelmann *et al.*, 2016,
78 Kasanke *et al.*, 2020, Slessarev *et al.*, 2020). Various approaches have been utilized to predict

79 switchgrass productivity, such as the use of Robel pole for ocular estimates (Schmer *et al.*, 2010),
80 process-based plant growth models (Behrman *et al.*, 2013, Brown *et al.*, 2000, Hartman *et al.*, 2011,
81 Kiniry *et al.*, 1996, McLaughlin *et al.*, 2006), empirical modeling (Jager *et al.*, 2010), and remote and
82 proximal sensing (Foster *et al.*, 2016, Gu *et al.*, 2015). Although remote sensing is a proven tool to
83 provide spatially comprehensive ecosystem activity (Churkina *et al.*, 2005), satellite-based
84 information is not readily available at finer temporal and spatial resolutions. Moreover, remote
85 sensing observations will not be available now for potential future production areas.

86 Information on ecosystem-level study of switchgrass productivity and its carbon dynamics in the
87 Southern Great Plain regions of the U.S. is lacking. Only a few studies have reported carbon
88 dynamics of switchgrass ecosystems for few years only based on EC measurements (Eichelmann *et*
89 *al.*, 2016, Liebig *et al.*, 2005, Skinner & Adler, 2010, Wagle & Kakani, 2014b, Wagle & Kakani,
90 2014c, Wagle *et al.*, 2015). The EC flux towers continuously measure ecosystem-level net exchange
91 of CO₂, H₂O, energy, and other trace gases between the land surface and the atmosphere. However,
92 EC systems provide measurements for their footprint areas or fetch lengths, which usually ranges
93 from 100 m to few kilometers depending on several factors, including EC tower height, wind speed,
94 and vegetation properties (Gockede *et al.*, 2004). Additionally, direct measurements of fluxes using
95 EC towers are cost-prohibitive and limited to flat topography with uniform vegetation only
96 (Baldocchi, 2008, Baldocchi, 2003). Thus, these site-level measurements need to be extrapolated or
97 upscaled at larger spatial scales to estimate the regional carbon balance (Wofsy *et al.*, 1993) and
98 facilitate carbon cycling research (Gilmanov *et al.*, 2005). In this paper, we developed empirical
99 models to derive switchgrass productivity during the growing season (April through October) using
100 EC-measured NEE from a switchgrass ecosystem and easily accessible time series meteorological
101 data from the Oklahoma Mesonet and validated the estimates of NEE to four different sites using
102 ancillary measures (e.g., NEE, biomass). Additionally, we characterize seamless switchgrass
103 productivity estimates for the potential switchgrass production areas in Oklahoma. This proposed
104 method can be implemented elsewhere for a regional prediction of switchgrass or any other
105 bioenergy production potential species.

106

107 **2 Materials and Methods**

108 **2.1 Net ecosystem CO₂ exchange measurements**

109 Eddy covariance measurements, equipped with a CSAT3 sonic anemometer (Campbell Scientific
110 Inc., Logan, UT, U.S.) and LI-7500 open-path infrared gas analyzer (IRGA, LI-COR Inc., Lincoln,
111 NE, U.S.), were taken in a switchgrass (cv. Alamo) field located at Oklahoma State University South
112 Central Research Station, Chickasha, Oklahoma (35° 2' 24" N, 97° 57' 0" W, 330 m above sea level)
113 after the first year of its establishment (2010). The EC data recorded at 10 Hz frequency were
114 processed using *EddyPro* software (LI-COR Inc., Lincoln, NE, U.S.) to compute 30-min eddy fluxes.
115 Data quality was assessed by the degree of energy balance closure [latent heat (LE) + sensible heat
116 (H)]/[net radiation (Rn) – soil heat flux (G)]. Energy balance closures of 0.77 and 0.83 were reported
117 for 2011 and 2012, respectively (Wagle and Kakani, 2014d), which were within the typical range for
118 EC experiments (Foken, 2008). The study area was under abnormally dry to exceptional drought
119 during the study period. Details on eddy flux measurements and data processing have been
120 extensively described previously (Wagle and Kakani, 2014c; a; Wagle *et al.*, 2014; Wagle *et al.*,
121 2015).

122 **2.2 Site description**

123 The State of Oklahoma was chosen as a study region given the presence of one of the foremost
124 mesoscale-level weather monitoring networks (Oklahoma Mesonet, <http://mesonet.org/>) that records
125 research-quality grade weather data. According to the Köppen-Geiger climate classification,
126 Oklahoma's climate has distinct zonation, with a humid subtropical climate in the east to a semi-arid
127 climate in the west (Kottek et al., 2006). The state covers the region bounded by 94° 29' 08.90" W–
128 103° 00' 06.631" W longitude and 33° 38' 17.7" N–37° 00' 00.473" N latitude. Topographic elevation
129 in Oklahoma ranges from 87 m near Little River to 1518 m above mean sea level on Black Mesa. A
130 distinct north-south temperature gradient and east-west precipitation gradient are present. The
131 average annual temperature is around 14°C along the northern border and 16.6 °C at the southern
132 border (see, http://climate.ok.gov/index.php/site/page/climate_of_oklahoma). Average annual
133 precipitation ranges from 432 mm in the far western panhandle to 1422 mm in the far southeast. The
134 state encompasses twelve level III eco-regions and forty-six level IV eco-regions (Woods et al.,
135 2005). Oklahoma has 14 million hectares of cropland area distributed throughout nine agricultural
136 districts (USDA, 2017a) (Northeast, Southeast, East Central, South Central, Central, North Central,
137 Southwest, West Central, and Panhandle). Forty-nine percent of the total cropland area is grass/
138 pasture, followed by 18% deciduous forest, and 11% wheat-grown areas. As per the recent
139 Conservation Reserve Program statistics (USDA, 2017b), 277,349 ha of land in Oklahoma are
140 enrolled in Conservation Reserve Program (<https://bit.ly/3Ftlulj>, accessed May 23, 2021). This
141 suggests there is an abundance of land for biomass feedstock production and a potential large market
142 for biofuels in Oklahoma.

143 The soil type at the flux tower siting was McClain silt loam (fine, mixed, super active, thermic,
144 Pachic Argiustolls) (Foster et al., 2015). The site where flux tower is located received a total of 525
145 and 673 mm precipitation during 2011 and 2012 compared to 30-year average (1981–2010) rainfall
146 of 896 mm. The aboveground switchgrass (cultivar Alamo) biomass data was manually harvested at
147 the end of the growing season (late September through early October) from Stillwater Agronomy
148 Research Station, Stillwater, Oklahoma (36°07'03.7"N 97°05'37.0"W); Wes Watkins Agricultural
149 Research and Extension Center, Lane, Oklahoma (34°18'17.9"N 96°00'12.3"W); South Central
150 Research Station, Chickasha, Oklahoma (35°02'38.9"N 97°54'50.2"W); and Southern Great Plains
151 Research Station, Woodward, Oklahoma (36°25'18.2"N 99°24'17.6"W) from 2011 to 2014. These
152 stations represent various ecoregions of Oklahoma (Tables

153 Table 1), and their mean monthly temperature and average monthly total precipitation are shown in
154 Fig. 1.

155 **2.3 Procuring and processing the Mesonet data**

156 Five-minute interval weather data for 110 environmental monitoring stations across Oklahoma (Fig.
157 2) were acquired from the Oklahoma Mesonet (Mesoscale network) from 2011 to 2014. The
158 automated weather stations collect statewide weather data, with a minimum of one site in each of
159 Oklahoma's seventy-seven counties to ensure spatial meteorological differences across landscapes
160 are captured well (Brock et al., 1995; McPherson et al., 2007). Most of the aboveground Mesonet
161 measurements are averaged over five minutes from measurements sampled every three seconds,
162 except for the barometer and the event driven rain gauge. Data included relative humidity (RH, %),
163 air temperature at 1.5 m (T_{air} , °C), solar radiation (S_{rad} , Wm^{-2}), liquid precipitation (Rain, mm), and
164 soil temperature under native vegetation at 5 cm (TS05, °C). Instruments used to measure these
165 variables are summarized in (Table 2). Data was checked thoroughly for missing and erroneous
166 observations and processed to calculate maximum, minimum, and average values for every 30-
167 minutes.

169 2.4 Deriving coefficients for NEE estimates

170 Empirical equations were developed based on EC measurements during the 2011 and 2012 growing
 171 seasons in a switchgrass field (8 ha) at the South-Central Research Station, Chickasha, Oklahoma.
 172 Light-saturated NEE (NEE_{sat}) was calculated as a function of air temperature (temperature ≥ 5.9 °C
 173 and PPFD $\geq 50 \mu \text{ mol m}^{-2} \text{ s}^{-1}$). Daytime respiration (DR) was calculated using a quadratic function of
 174 air temperature, whereas nighttime respiration (NR) was calculated using an exponential function of
 175 soil temperature. Temperature response curves were developed for NEE_{sat} , apparent quantum
 176 efficiency (α), DR, and NR. Based on these values, 30-minute NEE values were generated as a
 177 function of NEE_{sat} , photosynthetic photon flux density (PPFD), and α . We applied the same equations
 178 from April through October to the rest of the entire study period and locations.

179 The sign convention of NEE used in this study is that CO_2 uptake by the ecosystem is negative,
 180 whereas CO_2 release to the atmosphere is positive. The study window (i.e., growing season) was
 181 limited to the April 1-October 31 period for each year. We estimated values of PPFD ($\mu \text{ mol m}^{-2} \text{ s}^{-1}$ of
 182 photons with wavelengths of 0.4-0.7 $\mu \text{ m}$) using solar radiance values. In this study, a conversion
 183 factor of 1.892 was used to convert downwelling global solar radiation into photosynthetically active
 184 radiation (PAR) (Varlet-Grancher et al., 1981). The methodology evolves according to the following
 185 equations:

$$186 \quad PAR = 0.48 \times SI \quad (1)$$

$$187 \quad PPFD = 4.6 \times PAR \quad (2)$$

188 Following Tetens (1930), the saturation vapor pressure (e_s) (kPa) at a given air temperature, T (°C)
 189 was computed as:

$$190 \quad e_s = 0.6108 \exp \frac{17.27 \times T}{T + 237.3} \quad (3)$$

191 We calculated the saturation vapor pressure (e_s) at maximum (T_{max}) and minimum air
 192 temperature (T_{min}) by replacing T with T_{max} and T_{min} in the above equation.

$$193 \quad e_s = 0.5[e^0(T_{max}) + e^0(T_{min})] \quad (4)$$

194 Where $e^0(T_{max})$ and $e^0(T_{min})$ are the saturated vapor pressure at maximum and minimum
 195 temperature, respectively. The following equation recommended by Allen et al. (1998) was used to
 196 calculate actual vapor pressure (e_a) [kPa].

$$197 \quad e_a = \frac{e^0(T_{min}) \times \frac{RH_{max}}{100} + e^0(T_{max}) \times \frac{RH_{min}}{100}}{2} \quad (5)$$

199 Vapor pressure deficit (VPD) was calculated as a difference between saturation vapor
 200 pressure and actual vapor pressure.

201 Ecosystem respiration (ER) is the sum of autotrophic and heterotrophic respiration. Accurate
 202 quantification of ER is imperative for understanding switchgrass carbon dynamics as respiration
 203 emits a substantial proportion of daytime photosynthetic assimilates to the atmosphere. Measurement
 204 of CO₂ flux during nighttime by the EC system is underestimated due to weak mixing in less
 205 turbulence and presence of deep boundary layer; leading to systematic and methodological error
 206 (Wofsy et al., 1993; Ruimy et al., 1995; Lavigne et al., 1997). ER values were determined using the
 207 exponential temperature function developed by Lloyd and Taylor (1994) as:

$$208 \quad ER = R_0 e^{\beta T_s} \quad (6)$$

209 where R_0 ($\mu\text{mol CO}_2 \text{ m}^{-2} \text{ s}^{-1}$) is the base respiration at $T_s = 0$ °C, β ($^{\circ}\text{C}^{-1}$) is a constant related to
 210 temperature sensitivity coefficient (Q_{10}). The exponential model based on T_s explained 60% of the
 211 seasonal ER variation for the site when volumetric soil water content was $> 0.2 \text{ m}^3 \text{ m}^{-3}$ [$ER = 0.72 \times$
 212 $exp(0.08 \times T_s)$, $P < 0.0001$] (Wagle & Kakani, 2014a). Daily ER was also modeled as proposed by
 213 Reichstein et al. (2003) using daily average values of nighttime soil temperature and soil moisture as
 214 the main drivers of the nonlinear regression function.

$$215 \quad ER = R_{ref} \exp(a + b \times RSWC) \left(\frac{1}{T_{ref} - T_0} \right) \left(\frac{RSWC}{RSWC_{1/2} + RSWC} \right) \quad (7)$$

216 In this equation, R_{ref} ($\mu\text{mol m}^{-2} \text{ s}^{-1}$) is the ecosystem respiration under standard conditions (at
 217 $T_{ref} = 21$ °C; non-limiting water), T_{ref} ($^{\circ}\text{C}$) is the reference temperature, T_0 ($^{\circ}\text{C}$) is the lower
 218 temperature limit for the ER which was fixed at -46 °C as in the original model of Lloyd and Taylor
 219 (1994), and RSWC is the soil water content. $RSWC_{1/2}$ is the fraction of soil water content where half-
 220 maximal respiration occurs. This exponential temperature-respiration function could explain more
 221 than 50% of seasonal ER variation at soil moisture $> 0.20 \text{ m}^3 \text{ m}^{-3}$. We applied equation 8 to calculate
 222 ER throughout the growing season using soil temperature measurements as average of soil
 223 temperature records collected at 5 cm and 10 cm depths under the sod. Finally NEE data were
 224 partitioned into GPP and ER using the rectangular hyperbolic light-response function developed by
 225 Falge et al. (2001).

$$226 \quad NEE = \frac{\alpha \times GPP_{max}}{\alpha \times PPFD + GPP_{max} + ER} \quad (8)$$

227 where α is the apparent quantum yield, PPFD is photosynthetic photon flux density ($\mu\text{mol m}^{-2}$
 228 s^{-1}), GP_{max} is the maximum canopy CO₂ uptake rate ($\mu\text{mol m}^{-2} \text{ s}^{-1}$) at light saturation, and ER is
 229 respiration rate at zero PPFD. Limitation of higher VPD on photosynthesis was observed (Wagle and
 230 Kakani, 2014d) as Eq (7) failed to provide good fits for the NEE values. This problem was addressed
 231 by calculating GPP_{max} as the exponential decreasing function at high VPD, as suggested by Lasslop
 232 et al. (2010). A modification of the hyperbolic light response curve was imposed to account for the
 233 VPD limitation of GPP by replacing GPP_{max} with GP_0 .

$$234 \quad GPP_0 \exp(-k(VPD - VPD_0))_{0_{max}} \quad (9)$$

$$235 \quad GPP_0_{0_{max}} \quad (10)$$

236 where VPD_0 threshold was set to 1 kPa as in Lasslop et al. (2010). Additionally, k parameter
 237 was estimated using nonlinear least squared regression in SAS software (SAS Institute Inc., 2013,
 238 Cary, NC, U.S.). The NEE at light saturation (NEE_{sat}), contingent upon average temperature and
 239 PPFD values, was derived using the equations 11-13.

$$240 \quad \text{If } T_{avg} > 5.9, NEE_{sat} = \left((31.7659 - 0.8456 \times T_{avg} - 32.8766) - 2.006 \times \right. \\
 241 \quad \left. T_{avg} - 32.8766 \right); \text{ else } 0 \quad (11)$$

$$242 \quad \text{If } PPFD < 50, 0, \text{ else } NEE_{sat} \quad (12)$$

243 Light saturated NEE limited by VPD was computed as follows:

$$244 \quad NEE_{sat,VPD} = NEE_{sat} \times \exp(-0.2026 \times (VPD - 1)) \quad (13)$$

245 In addition, ER values were generated using the following equation:

$$246 \quad \text{If } PPFD \leq 50, ER = -0.7205 \times \exp(0.0814 \times TS_{05}); \\
 247 \quad \text{else, } ER = (-0.5135 \times T_{avg} + 0.115 \times T_{avg})^2 \quad (14)$$

248 Afterward, we computed α as following:

$$249 \quad \alpha = \left(0.0035 \times T_{avg} (0.00008 \times T_{avg}^2) \right) \quad (15)$$

250 Finally, the NEE values were calculated as following:

$$251 \quad \text{If } NEE_{sat,VPD} = 0, NEE_{final} = ER; \\
 252 \quad \text{else, } NEE_{final} = \frac{(NEE_{sat,VPD}) \times \alpha \times PPFD}{(NEE_{sat,VPD}) + PPFD + \alpha} \quad (16)$$

253 Total NEE ($\text{g CO}_2 \text{ m}^{-2}$) was computed using the following conversion factor:

$$254 \quad \frac{\sum NEE \times 1800}{22.6 \times 1000} \quad (17)$$

255 Gaps in the data were filled using average values immediately before and after the gap. We
256 calculated cumulative amounts of seasonal NEE that was sequestered per unit area.

257 **2.5 Identifying potential switchgrass establishment areas in Oklahoma**

258 According to the Conservation Reserve Program (CRP) - USDA Farm Service statistics of 2014, up
259 to 20% of the county area was under the CRP program in Oklahoma (Fig 3a). Especially, the
260 counties in western Oklahoma and Oklahoma Panhandle area (Texas, Cimarron, Beaver, Harper,
261 Ellis, and Grant) had most of the land area dedicated to the CRP. We aggregated six subclasses:
262 switchgrass, fallow, pasture, shrubland, and grassland as defined in the 2008-2014 USDA-NASS
263 Cropland Data Layer (CDL) to identify potential switchgrass production areas in Oklahoma. The
264 raster data were imported into ArcGIS and reclassified to show only potential switchgrass production
265 areas (Fig 3b).

266 As mentioned earlier, seasonal average NEE values were calculated for each of the Mesonet sites.
267 Calculated seasonal NEE values were then interpolated using ordinary kriging interpolation (Dhakal
268 et al., 2020). The mask identified for potential switchgrass production area was applied to the annual
269 NEE surface to generate seasonal switchgrass NEE across the state.

270 **2.6 Calibration and Validation**

271 We used three years (2011-2013) of EC measurements of CO₂ fluxes, the first two years of data for
272 developing the empirical equations, and the third year of data to validate the predictions made by our
273 empirical models. Conceptually, NEE can be linked to total biomass production. Hence, we used
274 end-of-season aboveground switchgrass biomass data as well to validate the NEE estimates with
275 measured aboveground switchgrass biomass from 2011 to 2013 in four locations (Lane, Stillwater,
276 Chickasha, and Woodward) in Oklahoma. Linear regression was used to compare paired
277 measurements of half-hourly EC-based NEE and half-hourly NEE estimates. To quantify the
278 accuracy of prediction, root mean square error (RMSE) was also reported, along with the coefficient
279 of determination and slope.

$$280 \text{ RMSE} = \sqrt{\sum_{i=1}^n \frac{(P_i - O_i)^2}{N}} \quad (19)$$

$$281 R^2 = \left(\frac{n(\sum XY) - (\sum x)(\sum y)}{\sqrt{[n\sum x^2 - (\sum x)^2][n\sum y^2 - (\sum y)^2]}} \right)^2 \quad (20)$$

282 **3 Results**

283 Pairwise comparisons of estimated NEE at half-hourly, monthly, and seasonal scales were made with
284 the measured NEE. For each year, we observed good agreements between the half-hourly measured
285 NEE and the estimated NEE, with R² values (*p* < 0.05) of 0.59, 0.63, and 0.63; and RMSE values of
286 4.78, 4.51, and 4.36 μmol CO₂ m⁻² s⁻¹, for 2011, 2012, and 2013 respectively (Fig. 4a). The
287 agreement was similar for 2012 and 2013, with R² values of 0.63 and slope of ~0.5. For all the years,
288 the slope of the regression line was less than one, suggesting underestimates of NEE values.

289 For each month of the growing season, there was a good agreement between the measured and
290 estimated half-hourly NEE values (R² values ranged between 0.52 and 0.74) (Fig. 4b). The
291 agreement was highest for May (R² = 0.74, slope = 0.46, *p* < 0.05) and lowest for October (0.52, slope

292 = 1.74, $p < 0.05$). Further, we aggregated monthly NEE values for each year and compared them
293 against the aggregated measured NEE values. A strong agreement between the monthly cumulative
294 measured and estimated NEE was observed for 2013, which was a wetter year ($R^2 = 0.91$, $p < 0.05$)
295 followed by a drier year 2012 ($R^2 = 0.81$, $p < 0.05$). However, the agreement was poor between the
296 measured and estimated monthly cumulative NEE values for 2011, which was a severe drought year
297 ($R^2 = 0.29$, $p < 0.05$). Contrarily, the slope of the regression line was closer to 1.0 for 2011 than 2012
298 and 2013. Looking at the sink-source status of the switchgrass ecosystem monthly, we observed that
299 the switchgrass ecosystem was a small source of CO_2 for July and August of 2011 and sink for the
300 rest of the months in the growing season but sink for CO_2 for the entire growing season of 2012 and
301 2013. Based on the estimated NEE values, May, and June (peak growth periods) had the highest
302 estimated NEE (negative sign convention) among the studied months across all three years.
303 However, a more accurate and complete NEE measurement and estimates of the true source-sink
304 status of the switchgrass ecosystem establishment warrants year-round, long-term studies.

305 Further, we computed seasonal NEE during 2011-2014 for Oklahoma State University's four
306 different research stations located at Stillwater, Lane, Chickasha, and Woodward (for site description,
307 refer to Table 1) using five-minute interval weather data for the Oklahoma Mesonet stations in
308 proximity to the research stations (STIL, LANE, CHIC, and WOOD) as mentioned earlier. For these
309 locations, we compared the seasonal NEE estimates with the end-of-the-season aboveground
310 switchgrass biomass collected from 2011 to 2014. Results showed strong agreements between the
311 measured aboveground switchgrass biomass and the seasonal carbon uptake by the switchgrass
312 ecosystem in all four stations ($R^2 > 0.93$, $p < 0.05$) (Fig. 6).

313 Upon observing a good agreement between seasonal NEE estimates and switchgrass aboveground
314 biomass production, we computed the NEE estimates for all active Oklahoma Mesonet stations. The
315 distribution of the seasonal NEE for each year is shown in Fig. 7. We generated seasonal C uptake
316 grids for the potential switchgrass production sites across the state of Oklahoma from 2011 to 2014
317 (Fig. 8). We used the ordinary kriging interpolation method to generate seasonal NEE raster surface
318 for those years. The year 2011 was a severe drought year and reported as the second driest year in
319 Oklahoma since 1925 (Shivers and Andrews, 2013). Statewide seasonal NEE for 2011 was recorded
320 as the lowest among the four ($278.5 \pm 154 \text{ g C m}^{-2}$). The effect of drought is visible in the annually
321 interpolated NEE surface (Fig. 8). The year 2014 had the highest seasonal NEE estimates (493 ± 181
322 g C m^{-2}).

323 For all the sites across 2011–2014, the average seasonal switchgrass NEE was estimated at around
324 $1870 \pm 703 \text{ g CO}_2 \text{ m}^{-2}$ ($5.1 \text{ Mg CO}_2 \text{ ha}^{-1}$). NEE values ranged from $-468 \text{ g CO}_2 \text{ m}^{-2}$ to -4093 g CO_2
325 m^{-2} for the Mesonet sites at Tipton, Oklahoma and Clayton, Oklahoma, respectively. The Mesonet
326 site at Tipton had temperature data missing for eight days, which resulted in the NEE estimates to be
327 the lowest among all the Mesonet sites.

328 4 Discussion

329 The concept for estimating carbon uptake per absorbed PAR has been demonstrated previously
330 (Monteith, 1972; Sinclair and Horie, 1989; Goetz and Prince, 1999). Based on the radiation use
331 efficiency concept, various models have been developed to simulate carbon exchange between the
332 atmosphere and terrestrial biosphere that account for spatiotemporal dynamics in the ecosystem for
333 both potential and natural vegetation (Kirschbaum et al., 2001; Fisher et al., 2014). In addition, use of
334 regression models have been also used to quantify the ecosystem CO_2 exchange. Zhang et al. (2011)
335 used piecewise regression model that included normalized difference vegetation index (NDVI),

336 phenological metrics, weather data, and soil water holding capacity to show that grasslands in the
337 U.S. Great Plains are net C sink (0.3 to 47.7 g C m⁻² yr⁻¹). Moreover, the ecological literature
338 contains a plethora of peer-reviewed scientific data highlighting the use of remotely and proximately
339 sensed vegetation production measurements and eddy flux measurements to estimate and upscale
340 NEE to a regional level (Emmerton et al., 2016; Reitz et al., 2021). For example, Asrar et al. (1984)
341 demonstrated that cumulative NDVI measurements through the growing season may be used to
342 obtain estimates of GPP. Because the coarse spatial resolution of the satellite derived measurements
343 has been identified as a source of error, coupling Landsat TM and Landsat ETM+ with flux tower
344 measurements using image fusion and regression tree approach was found to be effective for regional
345 NEE estimations (Fu et al., 2014). With improvement in high-resolution satellite sensors, shorter
346 satellite revisit time, high frequency weather data, and advanced data processing and machine
347 learning algorithms, remote sensing approach can be more appealing in regions with limited in-situ
348 observation networks (Sharma and Dhakal, 2021).

349
350 Recently, Liu et al. (2021) used various environmental variables (net radiation, soil water content,
351 soil temperature, precipitation, vapor pressure deficit, and wind speed) to predict NEE for 10
352 different biomes. The authors used trained XGBoost and Random Forest model to >10 years of
353 Fluxnet sites measurement across a wide range of biomes and obtained accurate prediction of NEE
354 for forest, savanna, and grassland ecosystems ($0.55 > R^2 < 0.81$) (Liu et al., 2021). Our approach also
355 relies completely on deriving relationships between the environmental variables such as air
356 temperature, soil temperature, and solar radiation to compute half-hourly NEE estimates. The
357 Oklahoma Mesonet records meteorological data at high temporal frequency (5-min intervals),
358 offering a unique possibility to produce empirical estimates of regional NEE of switchgrass when
359 extrapolated using measured NEE. Estimates of mean NEE across the Mesonet sites ranged from
360 2.78 ± 1.54 Mg C ha⁻¹ in 2011 to 4.93 ± 1.81 Mg C ha⁻¹ in 2014. The NEE estimates from the
361 semiarid sites of Oklahoma are similar to the EC flux measurements of NEE measured in a
362 switchgrass ecosystem in Central Illinois. (4.53 ± 0.2 Mg C ha⁻¹) (Zeri et al., 2011). Furthermore, the
363 NEE measurements acquired from a mature switchgrass stand in Southwestern Ontario for the year
364 2014 was 3.36 ± 0.38 Mg C ha⁻¹.

365
366 The temporal behaviour of NEE in the switchgrass ecosystem demonstrated seasonal and day-to-day
367 variations. Additionally, the spatiotemporal simulations illustrate the effect of microclimate
368 variability on the carbon balances is captured well for carbon budget related studies in switchgrass
369 ecosystem on a regional scale. This indicates that our approach using fine temporal resolution
370 meteorological forcings can capture and describe a range of variation of biophysical factors in
371 switchgrass ecosystems. Improvement in NEE estimates can be achieved by calibrating and
372 validating with site-specific flux and meteorological measurements.

373
374 Further inclusion of belowground biomass would significantly improve NEE estimates results at
375 localities. To our knowledge, there is no other empirical method that is robust across the interest of
376 scale of time and space, which simulates the switchgrass carbon uptake. In this study, the NEE
377 measured by EC technique at a location was extrapolated to quantify carbon sequestration potential
378 across potential switchgrass areas in Oklahoma using 30-minute averaged Mesonet data. As it has
379 been highlighted in the literature, upscaling of EC-based carbon fluxes to large regions has been
380 conducted using different approaches such as data-driven (empirical, statistical models) or data
381 assimilation approaches (ecosystem models, parameter estimation techniques) (Xiao et al., 2012).
382 Empirical estimates of net primary productivity for terrestrial plant communities were computed
383 from climatology-derived actual evapotranspiration (Rosenzweig, 1968). Gross primary production
384 (GPP) in the terrestrial ecosystems of the southern U.S. was estimated by scaling up leaf assimilation

385 rates of the shaded and sunlit canopy and factoring it with the daytime length (Tian et al., 2010).
386 Likewise, GPP modelling for boreal and temperate forest ecosystems was based on light use
387 efficiency, daily mean temperature, vapor pressure deficit (VPD), and soil water content (Makela et
388 al., 2008). In their study of carbon fluxes in ponderosa pine forest (*Arctostaphylos patula* and
389 *Purshia tridentata*), Law et al. (2001) also reported that Biome-BGC process model simulated carbon
390 budgets have been found to underestimate NEE compared to EC measurements.

391
392 Since our study was only limited to the growing season, source/sink dynamics for the entire year
393 were not captured. However, it is imperative to understand the responses of NEE to various climatic
394 conditions such as pluvial, drought, and normal years. Uncertainties in this study arise from
395 parameterizing the model with limited site and simplification of some of the ecosystem processes that
396 may not truly capture the exact variability of real phenomena. Most of the coefficients and constants
397 were generated from our calibration site. These values may vary spatially; therefore, additional
398 studies are necessary to investigate and reduce the uncertainty in the model's applicability. We only
399 conducted validation of NEE at the local level. Since this study was performed for potential
400 switchgrass growing areas, ground truth data for all the sites are not available. If the switchgrass
401 growing areas are large enough to be captured with satellite imagery, large-scale validation can be
402 performed using high-resolution remotely sensed data. There is also a potential for benefiting from
403 usage of current technology such as Uncrewed Aerial Vehicles (UAVs), which can capture the data
404 on-demand on a custom scale. However, that is beyond the scope of this study. Future studies should
405 focus on improving this empirical approach to include year-round estimates of NEE under various
406 climatic conditions.

407 **5 Conclusions**

408 The seasonal carbon balance of a switchgrass ecosystem was evaluated using an estimate of net
409 ecosystem CO₂ exchange (NEE). The models use radiation use efficiency approach, with air
410 temperature, soil temperature, vapor pressure deficit, and quantum use efficiency as modifying
411 factors. Empirical equations for estimating NEE of CO₂ in a switchgrass ecosystem were generated
412 and validated against eddy covariance tower measured NEE along with field data for switchgrass
413 biomass production and high frequency (5-min intervals) meteorological data from four locations.
414 Our results illustrate the importance of carbon balance model development on a temporal and spatial
415 scale. This approach can be used to compare direct carbon flux measurements or when flux
416 measurements data are unavailable for a better understanding of source-sink status of the switchgrass
417 ecosystems. The study could be helpful in adjusting cropping systems and management practices for
418 bioenergy production and understanding of carbon sequestration at a regional level. Undoubtedly,
419 with improved datasets at a range of scales and computing power, we will enhance our ability to
420 predict and capture spatial patterns of carbon exchange in switchgrass landscapes. However, we also
421 acknowledge the fact that such extrapolations should be done with care because of accompanying
422 uncertainties which require a thorough understanding of the subject matter. Given the findings here,
423 we recommend pursuing spatial modeling of NEE over a large spatial domain with additional field
424 measurements representative of that agroecological domain.

425 **6 Author Contributions**

426 KD, VGK, and PW: conceptualization. KD and VGK: formal analysis. VGK: fund acquisition. KD
427 and SS: original draft writing, data analysis, and visualization. KD, VGK, and PW: revision and
428 editing. All authors contributed to the article and approved the submitted version.

429 **7 Funding**

430 This research was funded by the USDA-NIFA, USDA-DOE Biomass Research and Development
431 Initiative, Grant No. 2009-1000606070. This manuscript is a contribution of the Oklahoma
432 Agricultural Experiment Station, Oklahoma State University, Stillwater, OK.

433 **8 Acknowledgments**

434 Oklahoma Mesonet data are provided courtesy of the Oklahoma Mesonet, which is jointly operated
435 by Oklahoma State University and the University of Oklahoma and funded through continued
436 support by the Oklahoman taxpayers. We also thank Evan Linde from Oklahoma State University
437 High Performance Computing Center for his support with creating and maintaining computing
438 resources used in this project.

439

440 **9 References**

- 441 Adler, P.R., Del Grosso, S.J., and Parton, W.J. (2007). Life-cycle assessment of net greenhouse-gas
442 flux for bioenergy cropping systems. *Ecol Appl* 17(3), 675-691. doi: 10.1890/05-2018.
- 443 Allen, R.G., Pereira, L.S., Raes, D.S., and Smith, M. (1998). "Crop evapotranspiration. Guidelines
444 for computing crop water requirements.", in: *FAO Irrigation and Drainage Paper 56*. (FAO,
445 Rome).
- 446 Asrar, G., Fuchs, M., Kanemasu, E.T., and Hatfield, J.L. (1984). Estimating Absorbed Photosynthetic
447 Radiation and Leaf Area Index from Spectral Reflectance in Wheat¹. *Agronomy Journal*
448 76(2), 300-306. doi: 10.2134/agronj1984.00021962007600020029x.
- 449 Baldocchi, D. (2008). Breathing of the terrestrial biosphere: lessons learned from a global network of
450 carbon dioxide flux measurement systems. *Australian Journal of Botany* 56(1), 1-26. doi:
451 10.1071/Bt07151.
- 452 Baldocchi, D.D. (2003). Assessing the eddy covariance technique for evaluating carbon dioxide
453 exchange rates of ecosystems: past, present and future. *Global Change Biology* 9(4), 479-492.
454 doi: 10.1046/j.1365-2486.2003.00629.x.
- 455 Behrman, K.D., Kiniry, J.R., Winchell, M., Juenger, T.E., and Keitt, T.H. (2013). Spatial forecasting
456 of switchgrass productivity under current and future climate change scenarios. *Ecol Appl*
457 23(1), 73-85. doi: 10.1890/12-0436.1.
- 458 Bigelow, D., Claassen, R., Hellerstein, D., Breneman, V., Williams, R., and You, C. (2020). " The
459 Fate of Land in Expiring Conservation Reserve Program Contracts, 2013-16 ".).
- 460 Brandes, E., McNunn, G.S., Schulte, L.A., Muth, D.J., VanLoocke, A., and Heaton, E.A. (2017).
461 Targeted subfield switchgrass integration could improve the farm economy, water quality,
462 and bioenergy feedstock production. *GCB Bioenergy* 10(3), 199-212. doi:
463 10.1111/gcbb.12481.
- 464 Brock, F.V., Crawford, K.C., Elliott, R.L., Cuperus, G.W., Stadler, S.J., Johnson, H.L., et al. (1995).
465 The Oklahoma Mesonet: A Technical Overview. 12, 5-19. doi: [https://doi.org/10.1175/1520-0426\(1995\)012<0005:TOMATO>2.0.CO;2](https://doi.org/10.1175/1520-0426(1995)012<0005:TOMATO>2.0.CO;2).
- 466
- 467 Brown, R.A., Rosenberg, N.J., Hays, C.J., Easterling, W.E., and Mearns, L.O. (2000). Potential
468 production and environmental effects of switchgrass and traditional crops under current and
469 greenhouse-altered climate in the central United States: a simulation study. *Agriculture,
470 Ecosystems & Environment* 78(1), 31-47. doi: 10.1016/s0167-8809(99)00115-2.

- 471 Churkina, G., Schimel, D., Braswell, B.H., and Xiao, X.M. (2005). Spatial analysis of growing
472 season length control over net ecosystem exchange. *Global Change Biology* 11(10), 1777-
473 1787. doi: 10.1111/j.1365-2486.2005.001012.x.
- 474 Demirer, R., Kutan, A.M., and Shen, F. (2012). The effect of ethanol listing on corn prices: Evidence
475 from spot and futures markets. *Energy Economics* 34(5), 1400-1406. doi:
476 10.1016/j.eneco.2012.06.018.
- 477 Dhakal, K., Kakani, V.G., Ochsner, T.E., and Sharma, S. (2020). Constructing retrospective gridded
478 daily weather data for agro - hydrological applications in Oklahoma. *Agrosystems,
479 Geosciences & Environment* 3(1). doi: 10.1002/agg2.20072.
- 480 Eichelmann, E., Wagner-Riddle, C., Warland, J., Deen, B., and Voroney, P. (2016). Carbon dioxide
481 exchange dynamics over a mature switchgrass stand. *GCB Bioenergy* 8(2), 428-442. doi:
482 10.1111/gcbb.12259.
- 483 Emmerton, C.A., St Louis, V.L., Humphreys, E.R., Gamon, J.A., Barker, J.D., and Pastorello, G.Z.
484 (2016). Net ecosystem exchange of CO₂ with rapidly changing high Arctic landscapes. *Glob
485 Chang Biol* 22(3), 1185-1200. doi: 10.1111/gcb.13064.
- 486 Falge, E., Baldocchi, D., Olson, R., Anthoni, P., Aubinet, M., Bernhofer, C., et al. (2001). Gap filling
487 strategies for defensible annual sums of net ecosystem exchange. *Agricultural and Forest
488 Meteorology* 107(1), 43-69. doi: 10.1016/S0168-1923(00)00225-2.
- 489 Fisher, J.B., Huntzinger, D.N., Schwalm, C.R., and Sitch, S. (2014). Modeling the Terrestrial
490 Biosphere. *Annual Review of Environment and Resources* 39(1), 91-123. doi:
491 10.1146/annurev-environ-012913-093456.
- 492 Foken, T. (2008). The energy balance closure problem: an overview. *Ecol Appl* 18(6), 1351-1367.
493 doi: 10.1890/06-0922.1.
- 494 Foster, A., Dhakal, K., Kakani, V., Gregory, M., and Mosali, J. (2015). Fine and Coarse Scale
495 Sampling of Spatial Variability within a Switchgrass Field in Oklahoma. *International Journal
496 of Plant & Soil Science* 6(5), 254-265. doi: 10.9734/ijpss/2015/16727.
- 497 Foster, A.J., Kakani, V.G., and Mosali, J. (2016). Estimation of bioenergy crop yield and N status by
498 hyperspectral canopy reflectance and partial least square regression. *Precision Agriculture*
499 18(2), 192-209. doi: 10.1007/s11119-016-9455-8.
- 500 Fu, D., Chen, B., Zhang, H., Wang, J., Black, T.A., Amiro, B.D., et al. (2014). Estimating landscape
501 net ecosystem exchange at high spatial-temporal resolution based on Landsat data, an
502 improved upscaling model framework, and eddy covariance flux measurements. *Remote
503 Sensing of Environment* 141, 90-104. doi: 10.1016/j.rse.2013.10.029.
- 504 Gelfand, I., Sahajpal, R., Zhang, X., Izaurrealde, R.C., Gross, K.L., and Robertson, G.P. (2013).
505 Sustainable bioenergy production from marginal lands in the US Midwest. *Nature* 493(7433),
506 514-517. doi: 10.1038/nature11811.
- 507 Gilmanov, T.G., Tieszen, L.L., Wylie, B.K., Flanagan, L.B., Frank, A.B., Haferkamp, M.R., et al.
508 (2005). Integration of CO₂ flux and remotely-sensed data for primary production and
509 ecosystem respiration analyses in the Northern Great Plains: Potential for quantitative spatial
510 extrapolation. *Global Ecology and Biogeography*. doi: 10.1111/j.1466-822X.2005.00151.x.
- 511 Gockede, M., Rebmann, C., and Foken, T. (2004). A combination of quality assessment tools for
512 eddy covariance measurements with footprint modelling for the characterisation of complex
513 sites. *Agricultural and Forest Meteorology* 127(3-4), 175-188. doi:
514 10.1016/j.agrformet.2004.07.012.
- 515 Goetz, S.J., and Prince, S.D. (1999). Modelling Terrestrial Carbon Exchange and Storage: Evidence
516 and Implications of Functional Convergence in Light-use Efficiency. *Advances in Ecological
517 Research* 28, 57-92. doi: [https://doi.org/10.1016/S0065-2504\(08\)60029-X](https://doi.org/10.1016/S0065-2504(08)60029-X).
- 518 Griffiths, M., Wang, X., Dhakal, K., Guo, H., Seethepalli, A., Kang, Y., et al. (2021). Interactions
519 among rooting traits for deep water and nitrogen uptake in upland and lowland ecotypes of

520 switchgrass (*Panicum virgatum* L.). *Journal of Experimental Botany*. doi:
521 10.1093/jxb/erab437.

522 Gu, Y., Wylie, B.K., and Howard, D.M. (2015). Estimating switchgrass productivity in the Great
523 Plains using satellite vegetation index and site environmental variables. *Ecological Indicators*
524 48, 472-476. doi: 10.1016/j.ecolind.2014.09.013.

525 Guo, Z., Gao, Y., Cao, X., Jiang, W., Liu, X., Liu, Q., et al. (2019). Phytoremediation of Cd and Pb
526 interactive polluted soils by switchgrass (*Panicum virgatum* L.). *Int J Phytoremediation*
527 21(14), 1486-1496. doi: 10.1080/15226514.2019.1644285.

528 Hartman, J.C., Nippert, J.B., Orozco, R.A., and Springer, C.J. (2011). Potential ecological impacts of
529 switchgrass (*Panicum virgatum* L.) biofuel cultivation in the Central Great Plains, USA.
530 *Biomass and Bioenergy* 35(8), 3415-3421. doi: 10.1016/j.biombioe.2011.04.055.

531 Jager, H.I., Baskaran, L.M., Brandt, C.C., Davis, E.B., Gunderson, C.A., and Wullschlegel, S.D.
532 (2010). Empirical geographic modeling of switchgrass yields in the United States. *GCB*
533 *Bioenergy* 2(5), 248-257. doi: 10.1111/j.1757-1707.2010.01059.x.

534 Kasanke, C.P., Zhao, Q., Bell, S., Thompson, A.M., and Hofmockel, K.S. (2020). Can switchgrass
535 increase carbon accrual in marginal soils? The importance of site selection. *GCB Bioenergy*
536 13(2), 320-335. doi: 10.1111/gcbb.12777.

537 Kiniry, J.R., Sanderson, M.A., Williams, J.R., Tischler, C.R., Hussey, M.A., Ocumpaugh, W.R., et
538 al. (1996). Simulating Alamo Switchgrass with the ALMANAC Model. *Agronomy Journal*
539 88(4), 602-606. doi: 10.2134/agronj1996.00021962008800040018x.

540 Kirschbaum, M.U.F., Carter, J.O., Grace, P.R., B.A., K., R.J., K., J.J., L., et al. (Year). "Brief
541 description of several ecosystem models for simulating net ecosystem exchange in Australia",
542 in: *Proc. NEE Worksh., Canberra.*, eds. M.U.F. Kirschbaum & R.B. Mueller: Coop. Res. Ctr.
543 for Greenhouse Accounting), pp. 8-29.

544 Kottek, M., Grieser, J., Beck, C., Rudolf, B., and Rubel, F. (2006). World map of the Koppen-Geiger
545 climate classification updated. *Meteorologische Zeitschrift* 15(3), 259-263. doi:
546 10.1127/0941-2948/2006/0130.

547 Langholtz, M.H. (2016). "Economic availability of feedstock. U.S. Department of Energy.
548 ORNL/TM-2016/160", in: *2016 Billion-ton report: Advancing domestic resources for a*
549 *thriving bioeconomy.* (Oak Ridge, TN).

550 Lasslop, G., Reichstein, M., Papale, D., Richardson, A.D., Arneth, A., Barr, A., et al. (2010).
551 Separation of net ecosystem exchange into assimilation and respiration using a light response
552 curve approach: critical issues and global evaluation. *Global Change Biology* 16(1), 187-208.
553 doi: 10.1111/j.1365-2486.2009.02041.x.

554 Lavigne, M.B., Ryan, M.G., Anderson, D.E., Baldocchi, D.D., Crill, P.M., Fitzjarrald, D.R., et al.
555 (1997). Comparing nocturnal eddy covariance measurements to estimates of ecosystem
556 respiration made by scaling chamber measurements at six coniferous boreal sites. *Journal of*
557 *Geophysical Research: Atmospheres* 102(D24), 28977-28985. doi: 10.1029/97JD01173.

558 Law, B.E., Thornton, P.E., Irvine, J., Anthoni, P.M., and Van Tuyl, S. (2001). Carbon storage and
559 fluxes in ponderosa pine forests at different developmental stages. *Global Change Biology*
560 7(7), 755-777. doi: DOI 10.1046/j.1354-1013.2001.00439.x.

561 Lee, D.K., Owens, V.N., and Doolittle, J.J. (2007). Switchgrass and soil carbon sequestration
562 response to ammonium nitrate, manure, and harvest frequency on conservation reserve
563 program land. *Agronomy Journal* 99(2), 462-468. doi: 10.2134/agronj2006.0152.

564 Liebig, M.A., Johnson, H.A., Hanson, J.D., and Frank, A.B. (2005). Soil carbon under switchgrass
565 stands and cultivated cropland. *Biomass and Bioenergy* 28(4), 347-354. doi:
566 10.1016/j.biombioe.2004.11.004.

- 567 Liu, J., Zuo, Y., Wang, N., Yuan, F., Zhu, X., Zhang, L., et al. (2021). Comparative Analysis of Two
568 Machine Learning Algorithms in Predicting Site-Level Net Ecosystem Exchange in Major
569 Biomes. *Remote Sensing* 13(12). doi: 10.3390/rs13122242.
- 570 Lloyd, J., and Taylor, J.A. (1994). On the Temperature-Dependence of Soil Respiration. *Functional*
571 *Ecology* 8(3), 315-323. doi: 10.2307/2389824.
- 572 Makela, A., Pulkkinen, M., Kolari, P., Lagergren, F., Berbigier, P., Lindroth, A., et al. (2008).
573 Developing an empirical model of stand GPP with the LUE approach: analysis of eddy
574 covariance data at five contrasting conifer sites in Europe. *Global Change Biology* 14(1), 92-
575 108. doi: 10.1111/j.1365-2486.2007.01463.x.
- 576 Marshall, C., Riffell, S.K., Miller, D.A., Hill, J.G., Evans, K.O., and Rush, S.A. (2017). Bird
577 response to intercropping switchgrass within a loblolly pine plantation. *Wildlife Society*
578 *Bulletin* 41(4), 659-665. doi: 10.1002/wsb.839.
- 579 Martinez - Feria, R., and Basso, B. (2020). Predicting soil carbon changes in switchgrass grown on
580 marginal lands under climate change and adaptation strategies. *GCB Bioenergy* 12(9), 742-
581 755. doi: 10.1111/gcbb.12726.
- 582 McLaughlin, S.B., Kiniry, J.R., Taliaferro, C.M., and De La Torre Ugarte, D. (2006). "Projecting
583 Yield and Utilization Potential of Switchgrass as an Energy Crop," in *Advances in Agronomy*.
584 Academic Press), 267-297.
- 585 McPherson, R.A., Fiebrich, C.A., Crawford, K.C., Elliott, R.L., Kilby, J.R., Grimsley, D.L., et al.
586 (2007). Statewide monitoring of the mesoscale environment: A technical update on the
587 Oklahoma Mesonet. *Journal of Atmospheric and Oceanic Technology* 24(3), 301-321. doi:
588 <https://doi.org/10.1175/Jtech1976.1>.
- 589 Mitchell, R.B., Lee, D.K., and Casler, M.D. (2014). "Switchgrass," in *Cellulosic Energy Cropping*
590 *Systems*, ed. D.L. Karlen. Wiley), 74–89.
- 591 Monteith, J.L. (1972). Solar Radiation and Productivity in Tropical Ecosystems. *The Journal of*
592 *Applied Ecology* 9(3). doi: 10.2307/2401901.
- 593 Ohlrogge, J., Allen, D., Berguson, B., Dellapenna, D., Shachar-Hill, Y., and Stymne, S. (2009).
594 Energy. Driving on biomass. *Science* 324(5930), 1019-1020. doi: 10.1126/science.1171740.
- 595 Reichstein, M., Rey, A., Freibauer, A., Tenhunen, J., Valentini, R., Banza, J., et al. (2003). Modeling
596 temporal and large-scale spatial variability of soil respiration from soil water availability,
597 temperature and vegetation productivity indices. *Global Biogeochemical Cycles* 17(4). doi:
598 10.1029/2003gb002035.
- 599 Reitz, O., Graf, A., Schmidt, M., Ketzler, G., and Leuchner, M. (2021). Upscaling Net Ecosystem
600 Exchange Over Heterogeneous Landscapes With Machine Learning. *Journal of Geophysical*
601 *Research: Biogeosciences* 126(2). doi: 10.1029/2020jg005814.
- 602 Robertson, G.P., Hamilton, S.K., Barham, B.L., Dale, B.E., Izaurrealde, R.C., Jackson, R.D., et al.
603 (2017). Cellulosic biofuel contributions to a sustainable energy future: Choices and outcomes.
604 *Science* 356(6345). doi: 10.1126/science.aal2324.
- 605 Rosenzweig, M.L. (1968). Net Primary Productivity of Terrestrial Communities - Prediction from
606 Climatological Data. *American Naturalist* 102(923p), 67-+. doi: 10.1086/282523.
- 607 Ruimy, A., Jarvis, P.G., Baldocchi, D.D., and Saugier, B. (1995). "CO₂ Fluxes over Plant Canopies
608 and Solar Radiation: A Review," in *Advances in Ecological Research*, eds. M. Begon & A.H.
609 Fitter. Academic Press), 1-68.
- 610 Schmer, M.R., Mitchell, R.B., Vogel, K.P., Schacht, W.H., and Marx, D.B. (2010). Efficient
611 Methods of Estimating Switchgrass Biomass Supplies. *BioEnergy Research* 3(3), 243-250.
612 doi: 10.1007/s12155-009-9070-x.
- 613 Sharma, S., and Dhakal, K. (2021). Boots on the Ground and Eyes in the Sky: A Perspective on
614 Estimating Fire Danger from Soil Moisture Content. *Fire* 4(3). doi: 10.3390/fire4030045.

615 Shivers, M.J., and Andrews, W.J. (2013). *Hydrologic drought of water year 2011 compared to four*
616 *major drought periods of the 20th century in Oklahoma: U.S. Geological Survey Scientific*
617 *Investigations Report 2013-5018*. U.S. Geological Survey and U.S. Department of Interior.

618 Shrestha, P., Bellitürk, K., and Gorres, J.H. (2019). Phytoremediation of Heavy Metal-Contaminated
619 Soil by Switchgrass: A Comparative Study Utilizing Different Composts and Coir Fiber on
620 Pollution Remediation, Plant Productivity, and Nutrient Leaching. *Int J Environ Res Public*
621 *Health* 16(7). doi: 10.3390/ijerph16071261.

622 Sinclair, T.R., and Horie, T. (1989). Leaf Nitrogen, Photosynthesis, and Crop Radiation Use
623 Efficiency: A Review. *Crop Science* 29(1), 90-98. doi:
624 10.2135/cropsci1989.0011183X002900010023x.

625 Skinner, R.H., and Adler, P.R. (2010). Carbon dioxide and water fluxes from switchgrass managed
626 for bioenergy production. *Agriculture Ecosystems & Environment* 138(3-4), 257-264. doi:
627 10.1016/j.agee.2010.05.008.

628 Slessarev, E.W., Nuccio, E.E., McFarlane, K.J., Ramon, C.E., Saha, M., Firestone, M.K., et al.
629 (2020). Quantifying the effects of switchgrass (*Panicum virgatum* L.) on deep organic C
630 stocks using natural abundance ¹⁴C in three marginal soils. *GCB Bioenergy* 12(10), 834-847.
631 doi: 10.1111/gcbb.12729.

632 Tetens, O. (1930). Über einige meteorologische Begriffe. *Z. Geophys* 6, 297-309.

633 Tian, H.Q., Chen, G.S., Liu, M.L., Zhang, C., Sun, G., Lu, C.Q., et al. (2010). Model estimates of net
634 primary productivity, evapotranspiration, and water use efficiency in the terrestrial
635 ecosystems of the southern United States during 1895-2007. *Forest Ecology and Management*
636 259(7), 1311-1327. doi: 10.1016/j.foreco.2009.10.009.

637 USDA (2014). "Conservation Reserve Program Annual Summary and Enrollment Statistics". United
638 States Department of Agriculture Farm Service Agency).

639 USDA (2017a). *2017 Census of Agriculture* [Online]. Available: <https://bit.ly/3ahShI7> [Accessed
640 Sep 1 2021].

641 USDA (2017b). *Conservation Reserve Program Statistics* [Online]. United States Department of
642 Agriculture Farm Service Agency. Available: <https://bit.ly/3Ftluj> [Accessed Sep 10 2021].

643 Varlet-Grancher, C., Chartier, M., Goose, G., and Bonhomme, R. (1981). Rayonnement utile pour la
644 photosynthèse des végétaux en conditions naturelles: Caractérisation et variations. *Acta*
645 *Aecologica Plantarum* 2, 189-202.

646 Wagle, P., and Kakani, V.G. (2014a). Confounding Effects of Soil Moisture on the Relationship
647 Between Ecosystem Respiration and Soil Temperature in Switchgrass. *Bioenergy Research*
648 7(3), 789-798. doi: 10.1007/s12155-014-9434-8.

649 Wagle, P., and Kakani, V.G. (2014b). Environmental control of daytime net ecosystem exchange of
650 carbon dioxide in switchgrass. *Agriculture Ecosystems & Environment* 186, 170-177. doi:
651 10.1016/j.agee.2014.01.028.

652 Wagle, P., and Kakani, V.G. (2014c). Growing season variability in evapotranspiration, ecosystem
653 water use efficiency, and energy partitioning in switchgrass. *Ecohydrology* 7(1), 64-72. doi:
654 10.1002/eco.1322.

655 Wagle, P., and Kakani, V.G. (2014d). Seasonal variability in net ecosystem carbon dioxide exchange
656 over a young Switchgrass stand. *Global Change Biology Bioenergy* 6(4), 339-350. doi:
657 10.1111/gcbb.12049.

658 Wagle, P., Kakani, V.G., and Huhnke, R.L. (2015). Net ecosystem carbon dioxide exchange of
659 dedicated bioenergy feedstocks: Switchgrass and high biomass sorghum. *Agricultural and*
660 *Forest Meteorology* 207, 107-116. doi: 10.1016/j.agrformet.2015.03.015.

661 Wagle, P., Xiao, X., Torn, M.S., Cook, D.R., Matamala, R., Fischer, M.L., et al. (2014). Sensitivity
662 of vegetation indices and gross primary production of tallgrass prairie to severe drought.
663 *Remote Sensing of Environment* 152, 1-14. doi: 10.1016/j.rse.2014.05.010.

- 664 Wofsy, S.C., Goulden, M.L., Munger, J.W., Fan, S.M., Bakwin, P.S., Daube, B.C., et al. (1993). Net
665 Exchange of CO₂ in a Mid-Latitude Forest. *Science* 260(5112), 1314-1317. doi:
666 10.1126/science.260.5112.1314.
- 667 Woods, A.J., Omernik, J.M., Butler, D.R., Ford, J.G., Henley, J.E., Hoagland, B.W., et al. (2005).
668 *Ecoregions of Oklahoma (color poster with map, descriptive text, summary tables, and*
669 *photographs): Reston, Virginia, U.S. Geological Survey (map scale 1:1,250,000).*
- 670 Wright, L. (2007). "Historical perspective on how and why switchgrass was selected as a "model"
671 high-potential energy crop".).
- 672 Xiao, J.F., Chen, J.Q., Davis, K.J., and Reichstein, M. (2012). Advances in upscaling of eddy
673 covariance measurements of carbon and water fluxes. *Journal of Geophysical Research-*
674 *Biogeosciences* 117. doi: 10.1029/2011jg001889.
- 675 Zeri, M., Anderson-Teixeira, K., Hickman, G., Masters, M., DeLucia, E., and Bernacchi, C.J. (2011).
676 Carbon exchange by establishing biofuel crops in Central Illinois. *Agriculture Ecosystems &*
677 *Environment* 144(1), 319-329. doi: 10.1016/j.agee.2011.09.006.
- 678 Zhang, L., Wylie, B.K., Ji, L., Gilmanov, T.G., Tieszen, L.L., and Howard, D.M. (2011). Upscaling
679 carbon fluxes over the Great Plains grasslands: Sinks and sources. *Journal of Geophysical*
680 *Research* 116(G3), n/a-n/a. doi: 10.1029/2010jg001504.

681

682 **Tables**

683 **Table 1.** Characteristics of the switchgrass grown fields, including soils (USDA, 2017), the United States Environmental Protection
 684 Agency (EPA) ecoregion (Level IV ecoregion of are shown in parenthesis), and the United States Department of Agriculture Plant
 685 Hardiness Zone.

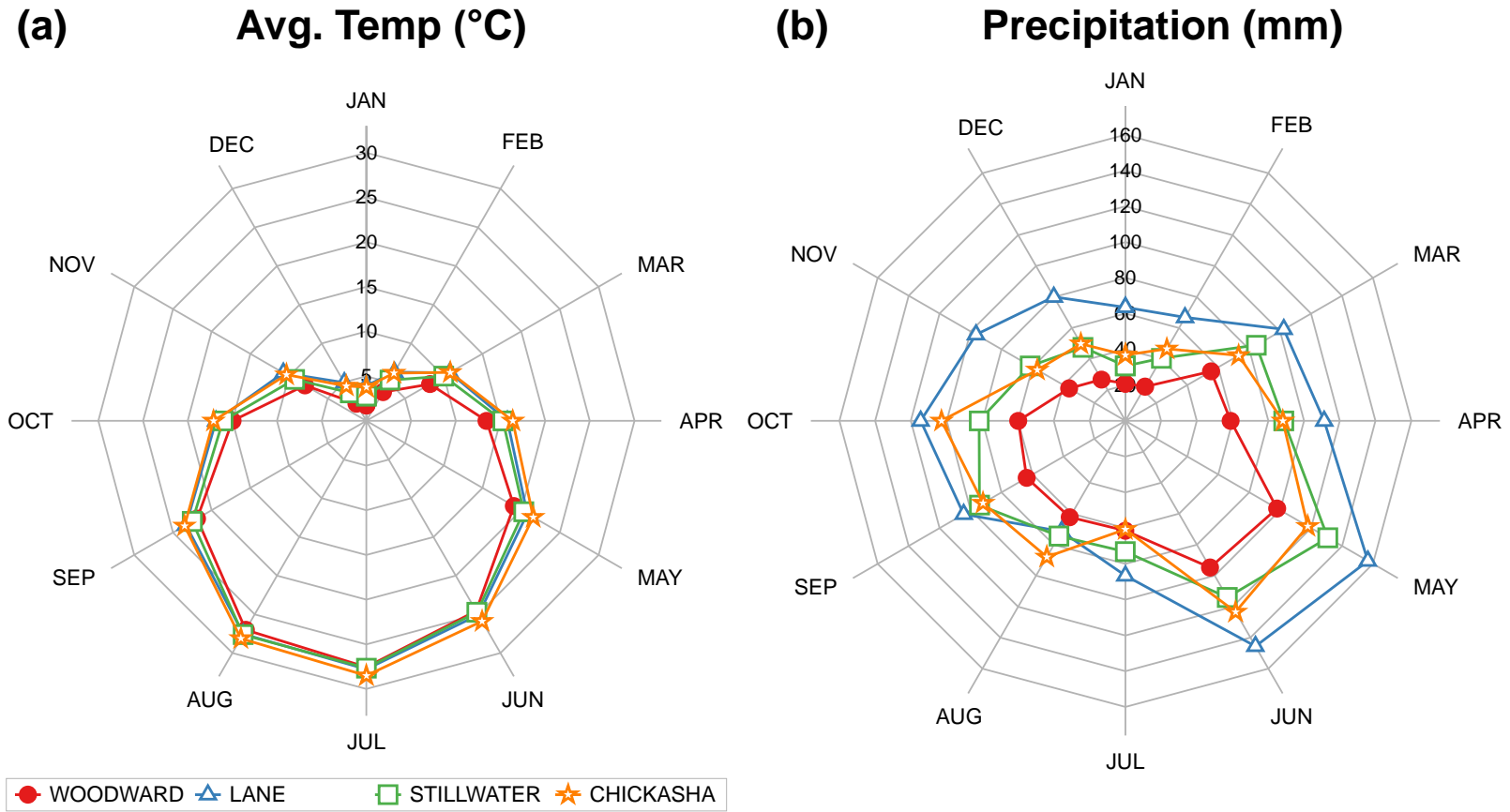
Site	Soil name	Dominant taxonomic classification	EPA Ecoregion	USDA Plant Hardiness Zone
Lane	Bernow	Fine-loamy, siliceous, active, thermic Glossic Paleudalfs	South Central Plains (35d)	7b
Stillwater	Easpur	Fine-loamy, mixed, superactive, thermic Fluventic Haplustolls	Central Great Plains (27o)	7a
Chickasha	Dale McLain	a) Fine-silty, mixed, superactive, thermic Pachic Haplustolls b) Fine, mixed, superactive, thermic Pachic Argiustolls	Central Great Plains (27d)	7 7a
Woodward	a) Devol b) Eda	a) Coarse-loamy, mixed, superactive, thermic Typic Haplustalfs b) Mixed, thermic Lamellic Ustipsaments	Central Great Plains (27q)	6b

Table 2 Summary of the sensors used in the Oklahoma Mesonet network.

Variable	Sensor	Unit	Accuracy
Air Temperature at 1.5 m	Thermometrics Air Temperature	°C	± 0.5 °C
Rainfall	Met One Tipping-Bucket	mm	±5% over the range of 0 to 5 cm hr ⁻¹
Soil Temperature, under sod (5 cm)	Stainless steel encased 10K thermistor probe, thermocouple sensor	°C	±0.5 °C
Solar Radiation	LI-200S Pyranometer	W m ⁻²	±5%

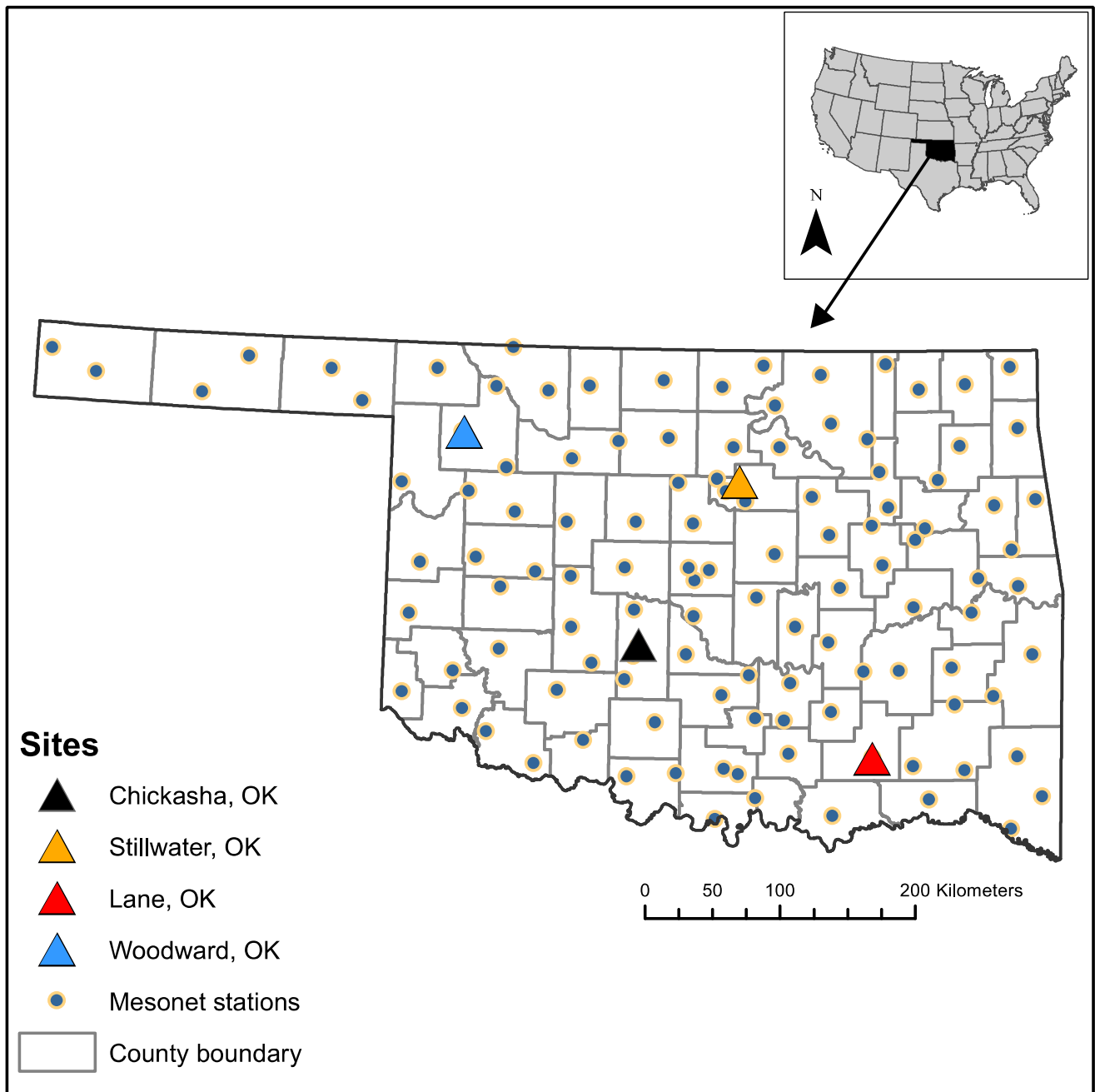
687

688



690

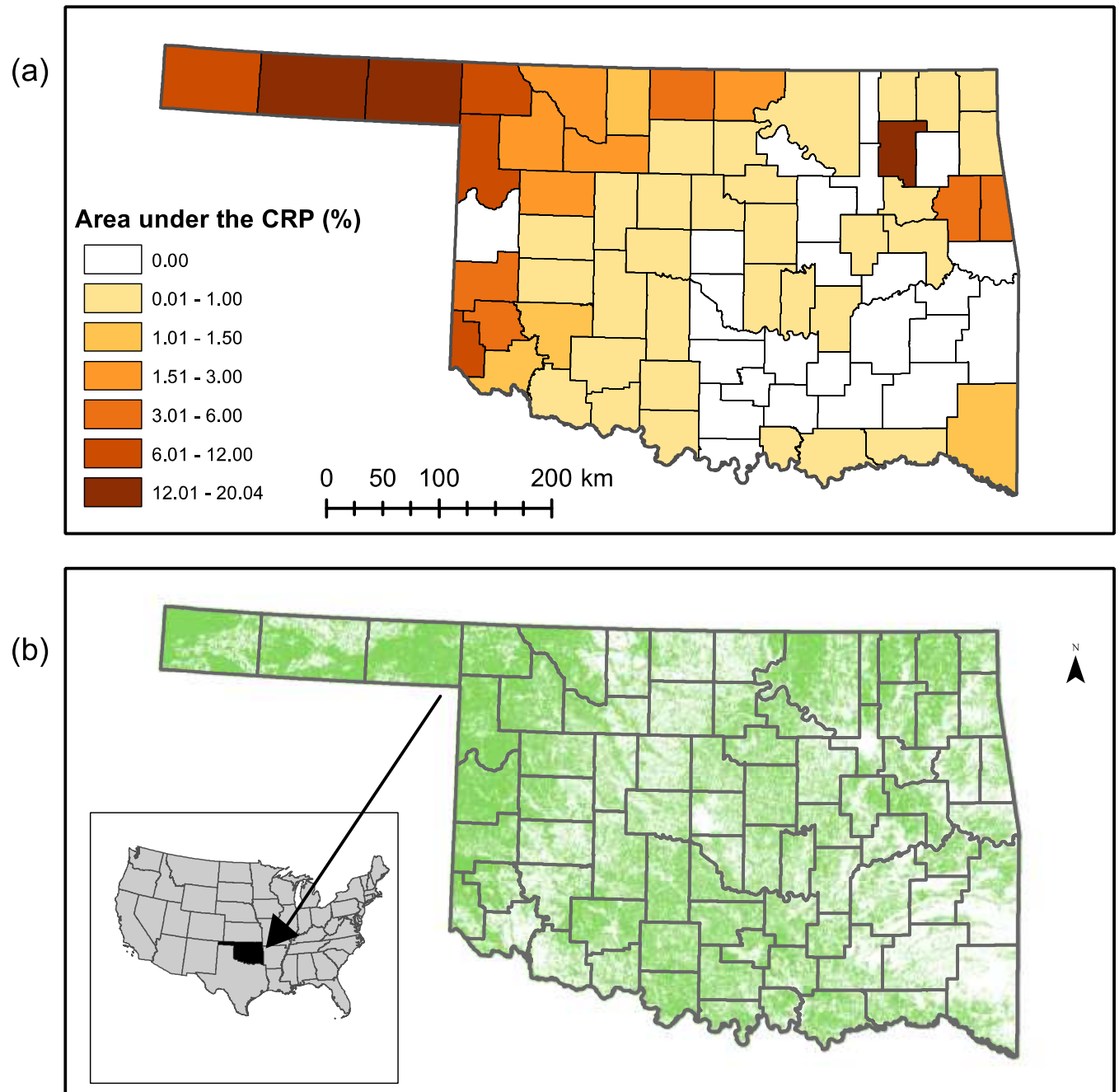
691 **Fig. 1.** Mean monthly temperature (°C) (a) and average total precipitation (mm) for four study locations (Lane, Stillwater, Chickasha, and
 692 Woodward) based on 30-year climate normal.



693

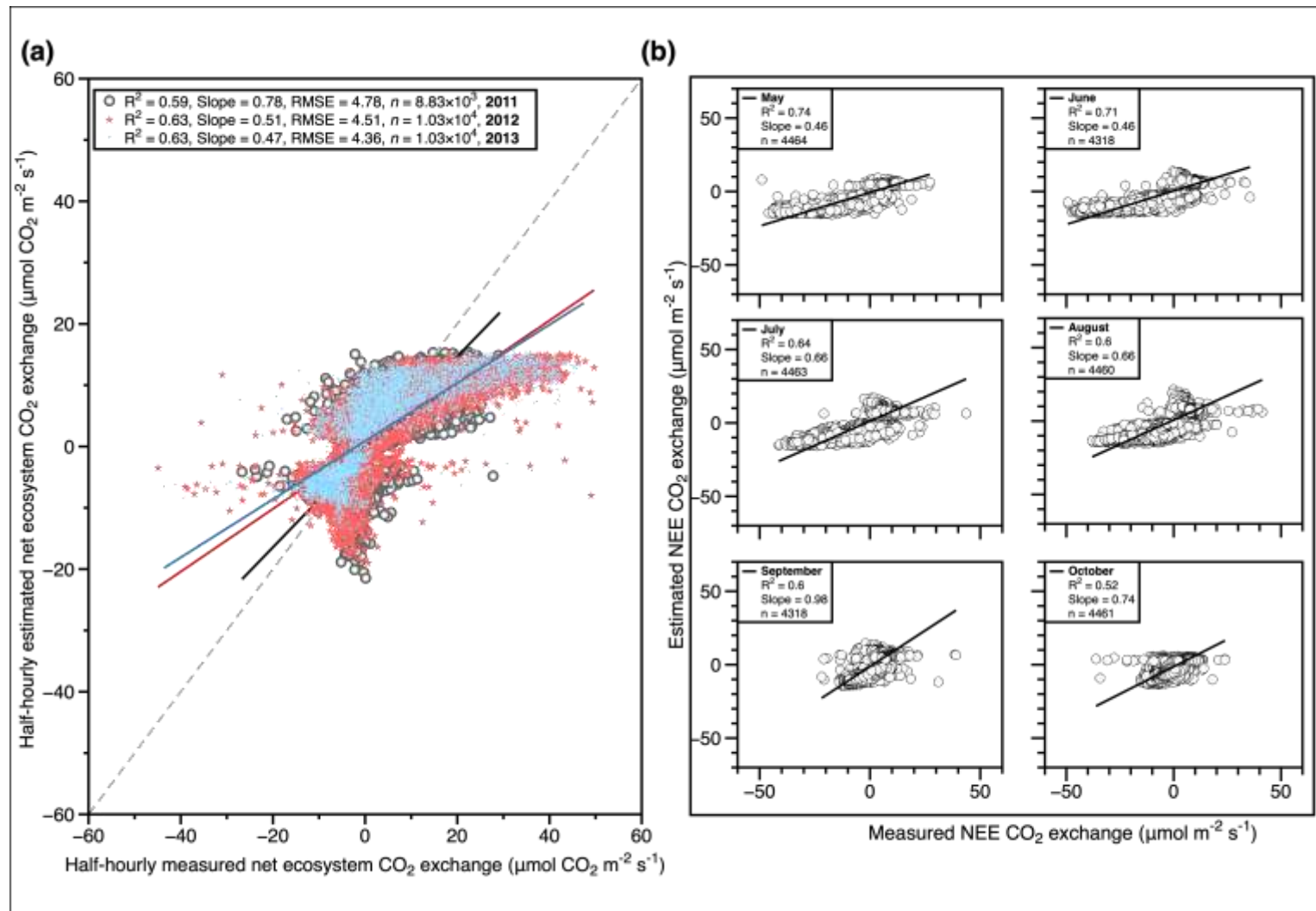
694
695
696
697
698

Fig. 2. Mesonet site distribution across Oklahoma. The black triangle is the site in Chickasha, Oklahoma, where empirical models were derived using Eddy flux measurements. Blue, yellow, and red triangles are the field-based biomass data acquired at Woodward, Stillwater, and Lane, respectively. Polar plots of (a) average temperature and (b) precipitation for Woodward, Lane, Stillwater, and Chickasha, respectively.



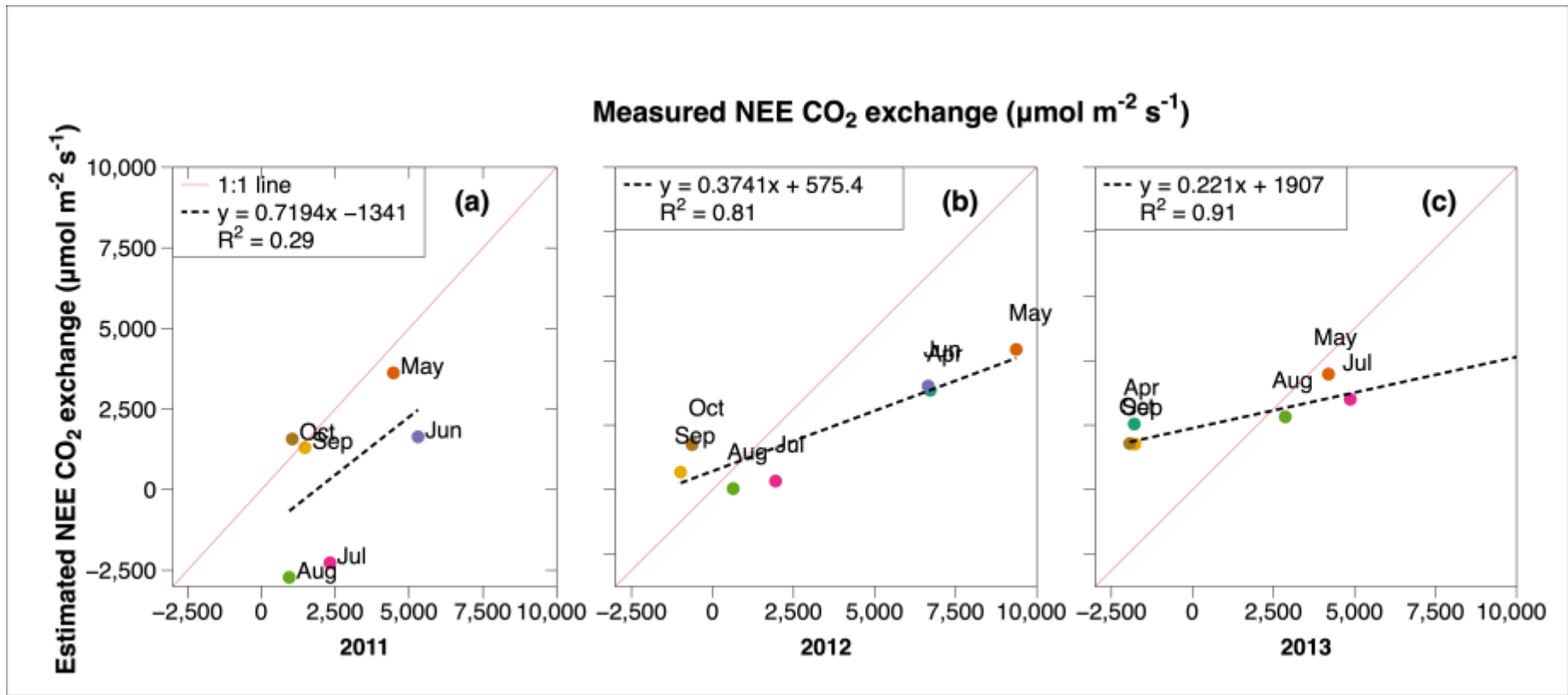
699

700 **Fig. 3.** Spatial distribution of the percentage of county area dedicated to the Conservation Reserve
 701 Program (CRP) in Oklahoma (a). Potential switchgrass production areas estimated by reclassifying
 702 the USDA-NASS Crop Data Layer 2008–2014 (b).



703

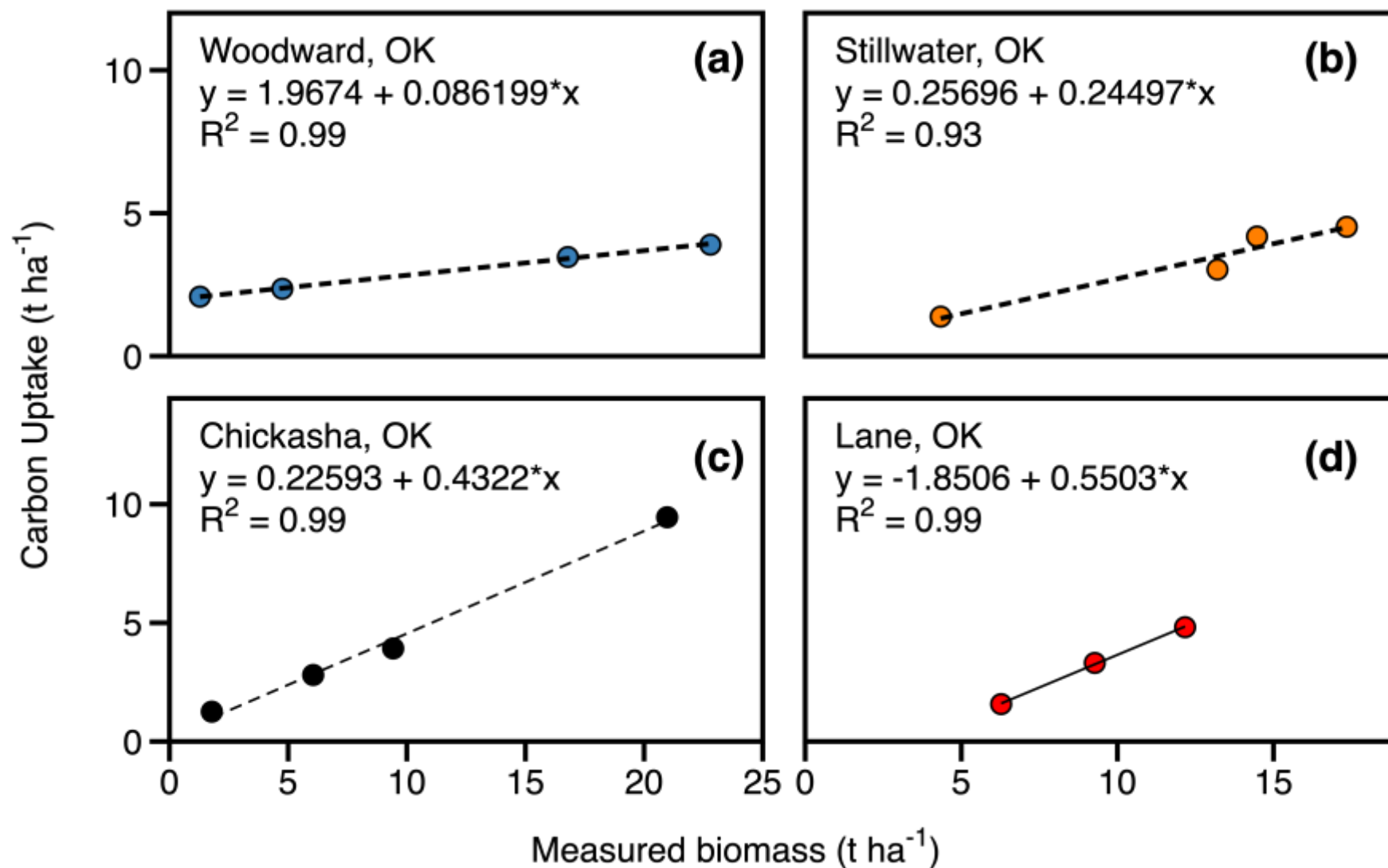
704 **Fig. 4.** (a) Comparison of empirical estimates of half-hourly net ecosystem CO₂ exchange (NEE) with measured half-hourly NEE for 2011,
 705 2012, and 2013. The dotted black line represents a 1:1 relationship. (b) Comparison of half-hourly NEE with empirical NEE estimates for
 706 each of the individual months (May through October) of the active growing season.



707

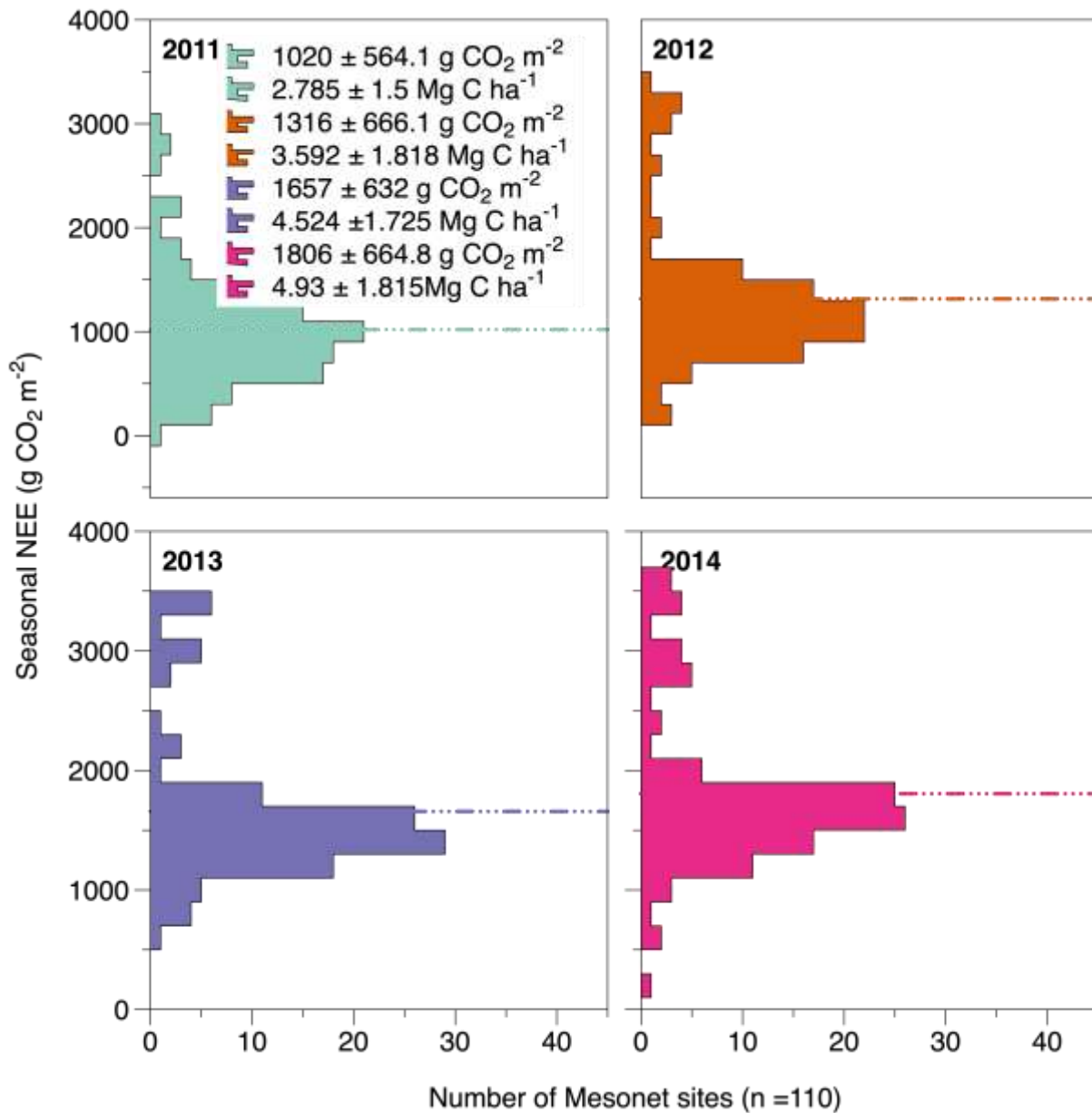
708 **Fig. 5.** Relationship between cumulative monthly measured and estimated net ecosystem CO₂ exchange (NEE) for Chickasha, Oklahoma in
 709 2011, 2012, and 2013.

710



711

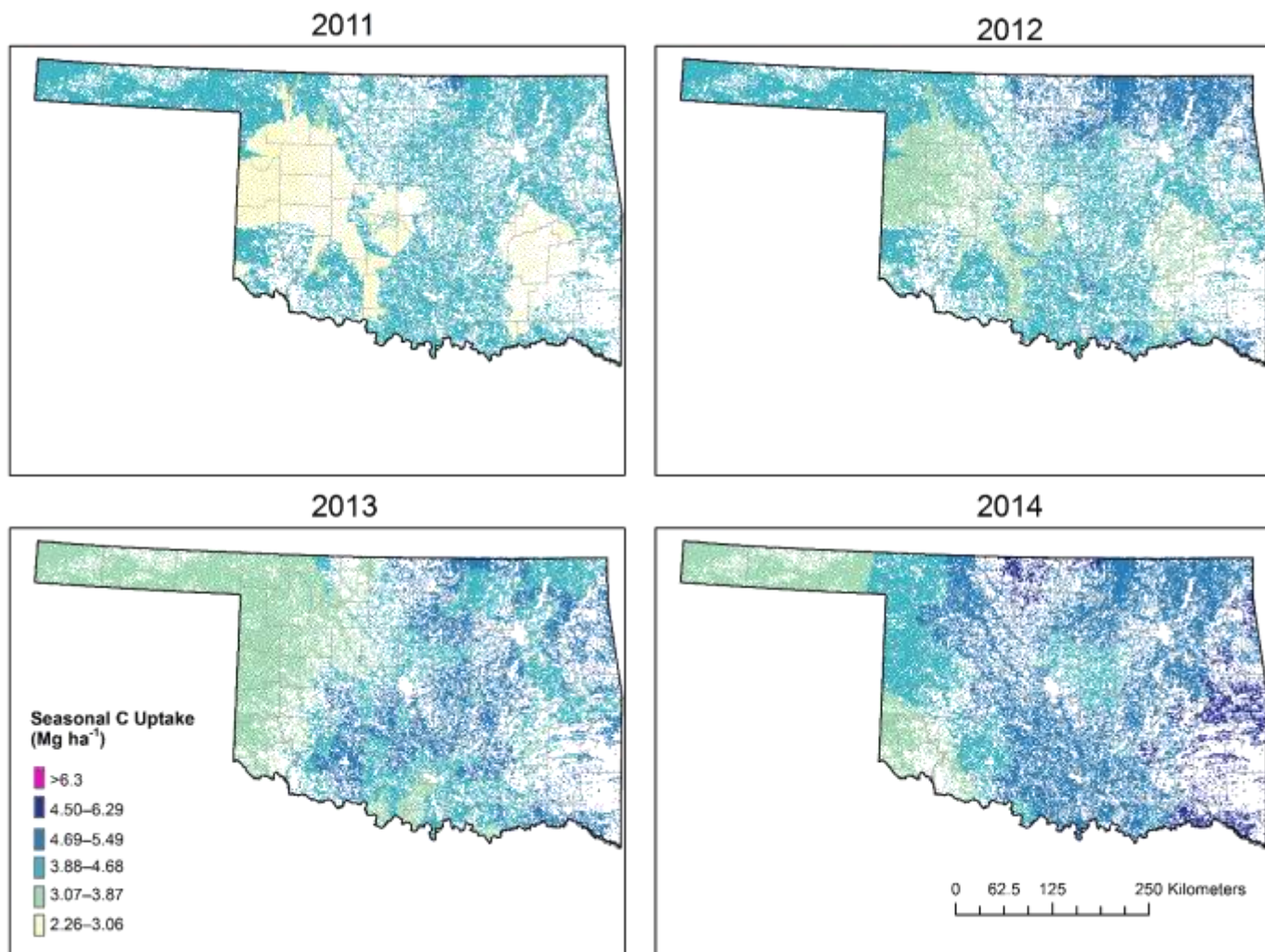
712 **Fig. 6.** Relationship between seasonal (April–October) carbon uptake (net ecosystem CO₂ exchange, t ha⁻¹) by switchgrass ecosystem and
 713 end-of-season aboveground switchgrass biomass for (a) Woodward, Oklahoma, (b), Stillwater, Oklahoma (c) Chickasha, Oklahoma, and (d)
 714 Lane, Oklahoma for 2011–2014. Biomass yield for Lane, Oklahoma for 2014 was not available.



716

717 **Fig. 7.** Histogram of the seasonal net ecosystem CO_2 exchange (NEE) for the Mesonet sites for 2011-
 718 2014. Dashed lines represent the mean for the given year, and the legend shows the mean \pm standard
 719 deviation of the seasonal NEE values across the Oklahoma Mesonet sites.

720



721

722 **Fig. 8.** Spatial explicit prediction of growing season net ecosystem CO₂ exchange (NEE) in a
 723 switchgrass ecosystem from 2011 to 2014 in a theoretical switchgrass production area across
 724 Oklahoma.

725